*Desalination and Water Treatment*
www.deswater.com

doi: 10.5004/dwt.2023.30104

314 (2023) 24–34
December

# Valorization of bovine bones for the development of bio-ceramic ultrafiltration membranes for wastewater treatment

Maryam Mallek[a], Hafed Elfeki[a], Victoria Salvadó[b,*]

[a]*Laboratory of Materials Science and Environment, Faculty of Science of Sfax, University of Sfax, Route de la Soukra Km 3.5, BP 1171, 3000, Sfax, Tunisia, emails: mallek.mariem87@gmail.com (M. Mallek), hafed.elfeki@gmail.com (H. Elfeki)*
[b]*Department of Chemistry, University of Girona, M. Aurèlia Capmany, 69, 17003 Girona, Spain, email: victoria.salvado@udg.edu*

Received 19 July 2023; Accepted 13 October 2023

**ABSTRACT**

The present study focuses on the use of hydroxyapatite from bovine bones to form a flat porous ceramic support for low-cost ultrafiltration membranes. The chemical composition, structure and particle size of the material and support were characterized by X-ray fluorescence (XRF), X-ray diffraction (XRD), energy-dispersive X-ray spectroscopy (EDX), Fourier-transform infrared spectroscopy (FTIR), thermogravimetry (TGA), differential scanning calorimetry (DSC), scanning electron microscopy (SEM), and nitrogen adsorption/desorption isotherm (BET) techniques. Bovine bone powder treated at high temperature was mixed with two organic additives and water allowing for extrusion shaping. The membrane prepared with 92 wt.% bovine bone powder and 8 wt.% additives at the sintering temperature of 1,350°C has an average pore size of 20 nm, a high mechanical strength (16.1 Mpa) and high chemical resistance (total weight loss of 1.86%). The ultrafiltration membrane with a stable flux of 470.49 L $h^{-1}$ $m^{-2}$ $bar^{-1}$ was applied to treat a pharmaceutical industry effluent resulting in removals of 73% of the chemical oxygen demand, 97% of turbidity, 48.15% of conductivity, 42% of BOD, and more than 99.3% of iron and 75.6% of zinc. This study shows that ultrafiltration membranes prepared from bovine bone are efficient for the treatment of industrial wastewaters.

*Keywords:* Biomaterials; Bovine bones; Membrane; Ultrafiltration; Wastewater treatment; Heavy metals; Hydroxyapatite

## 1. Introduction

In recent years, the use of membrane technology has received considerable attention both by the research community and industry due to its great efficiency in many separation processes together with its cost-effectiveness and low energy consumption [1].

Membrane technologies are commonly used in various sectors, including the chemical, food, and biotechnology industries, and wastewater treatment [2]. Membranes act as a physical barrier and so the size exclusion mechanism is of paramount importance in the membrane separation process. Different types of porous and thin-film composite membranes can be used for water/wastewater treatment. These include low pressure-driven membrane processes (microfiltration (MF), ultrafiltration (UF), high pressure-driven membrane processes (nanofiltration (NF) and reverse osmosis (RO)), osmotic pressure-driven membrane process (forward osmosis (FO)), and others (electrodialysis (ED), etc. Microfiltration (MF), pore size ranging from 0.1 to 10 microns, and ultrafiltration (UF), ranging from 0.001 to 0.1 microns, membranes are used for the elimination of suspended solids, colloids, bacteria, and viruses [3]. In selecting a suitable membrane, parameters such as the amount of wastewater, the targeted species and the operating conditions need to be taken into account.

* Corresponding author.

Membranes made from ceramic and polymeric materials are commercialized worldwide, although the low price of polymeric membranes makes them particularly attractive for water treatment applications. However, polymeric membranes have the drawbacks of short lifetime, easy fouling, and poor chemical and mechanical stability. Given these problems, there is now heightened interest in improving ceramic membranes [4], which can provide high thermal and chemical stability, resistance to high pressures, the ability to operate in harsh chemical conditions, and catalytic properties resulting from their intrinsic nature [5,6]. The cost of ceramic membranes has until now been relatively high due to the limited choice of materials available and so an intense search is now underway for new less costly alternatives from inorganic sources that are abundant and do not require firing temperatures that are as high as those needed for metal oxide materials [7–9]. Materials tested include cheaper raw materials such as natural phosphate [10], natural clay [8,11–13], natural pozzolana [14], animal bone [15], cordierite [16,17] and kaolin [18–20]. Recently, low-cost microporous ceramic membranes have been successfully manufactured from clayey resources blended using bio-based porosifying additives (i.e., woodworking waste and rice husk) [21].

Waste animal bones have been widely explored as an alternative source for preparing ceramic membranes given that they consist of hydroxyapatite (HAp) [15]. Several synthesizing routes have been introduced to produce HAp from waste animal bones, such as precipitation [22], a hydrothermal process [23], and thermal treatment [24]. Of these methods, thermal treatment is the most commonly used to prepare HAP and has been applied in the production of membranes [25].

The aim of the present study is to prepare low-cost ceramic membranes based on bovine bone waste, which is produced in large quantities in Tunisia as well as all over the world in general. The powder is used in the manufacturing of a membrane support, allowing the removal of contaminants from industrial pharmaceutical wastewater. This work also aims to establish the analytical methods that will be required to assess the safety of the final product. The characteristics of the additives and their influence on the formulation of a good support that is similar to synthetic hydroxyapatite are investigated as are the microstructures, porosity, shrinkage, mechanical strength and the chemical stability of the final support.

## 2. Experimental

### 2.1. Materials and preparation

Fresh bones, which were provided by butcher shops in the Sfax region in central Tunisia, were cut into small pieces and cleaned well. The bones were then boiled in water for 30 min to disinfect them and eliminate fat, tissue and bone marrow. After cooling, the bones were dried at 100°C. The bones were then ground down with a ceramic mortar, passed through a 125-mesh sieve and then calcined at 800°C for 2 h. Corn starch (RG 03408, Cerestar) was added to form pores and methylcellulose (Dow Chemical Company) was used as a plasticizer and binder.

### 2.2. Synthesis of the support

Fig. 1 illustrates the preparation of the membrane support using the sintering technique. Natural hydroxyapatite powder was first dry mixed for 30 min before the addition of the organic additives to avoid potential agglomerations and obtain a homogeneous powder. The organic additives methylcellulose and corn starch were used to improve the rheological properties of the paste, so permitting shaping by calendering.

The ceramic paste was prepared by adding 65–70 mL of water for each 200 g of powder. The paste was then stored in a closed box for 24 h in conditions of high humidity to improve its rheological properties by avoiding premature drying and ensuring complete diffusion of the water and organic additives. The final samples were obtained by calendering the paste, giving flat disk supports with a diameter of 6 cm and a thickness of 5 mm. The dough of the support was flattened between two rollers, using a Lloyd Instruments machine (Ametek Inc.).

After drying at room temperature for 24 h, the supports were sintered in a furnace below its melting point, at 1,350°C until the particles adhered to one other (Fig. 2).

### 2.3. Preparation of synthetic hydroxyapatite

The calcined bovine bone obtained was compared with a synthetic hydroxyapatite prepared following a slightly modified co-precipitation method [26]. This method consisted in the stepwise addition, every 3 min, of 5 mL of a solution A into a solution B over a period of 3 h at a temperature between 80°C–100°C. Solution A was composed of calcium nitrate tetrahydrate, $Ca(NO_3)4H_2O$:2.361 g

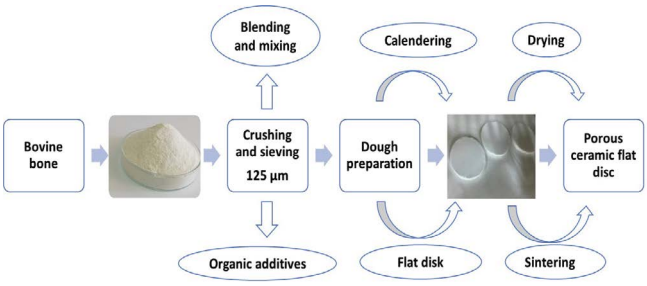


Fig. 1. Schematic diagram for the preparation of natural HAp derived from bovine bone.

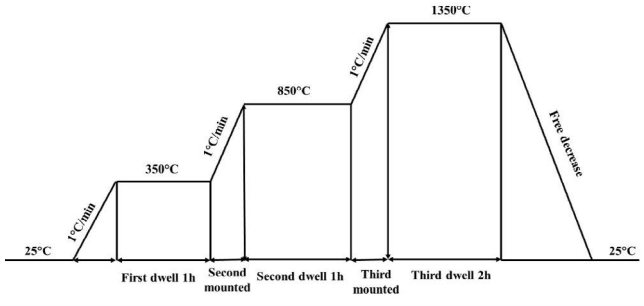


Fig. 2. Sintering programme of the extruded supports.

dissolved in 333 mL of distilled water whereas solution B consisted of ammonium phosphate, $(NH_4)_2HPO_4$:0.79 g dissolved in 842 mL of water. The alkaline medium was maintained to a pH range between 9 and 10 by adding 5 mL of ammonia, $NH_3$, every 30 min. After heating to 100°C, the resulting solution of the two mixtures is left at reflux for 1 h and then filtered while hot through a Büchner funnel before being washed with distilled water. Finally, the precipitate is dried for 24 h in an oven at 140°C.

### 2.4. Preparation of the ultrafiltration layer

A slip casting method was made by combining 10 wt.% of the same natural powder (≤100 μm), 60 wt.% water, and 30 wt.% polyvinyl alcohol (PVA). The flat support was coated with a bovine bone powder suspension using a spin-coating method. The membrane was then dried at room temperature overnight. Afterwards, the membrane was heated at a temperature of 200°C for 2 h to completely eliminate PVA before sintering at 1,350°C.

### 2.5. Characterization techniques

The phase and crystallinity information of samples was obtained using an X-ray diffractometer (XRD, Bruker AXS, Model D8 Avance) equipped with a secondary monochromator (to suppress background fluorescence radiation and Kβ radiation) and a copper anticathode tube over the Bragg angle ranging from 10° to 60°. The particle size was analyzed using a LS 13 320 laser diffraction particle size analyzer (Beckman Coulter). The measurements of the specific surface area and the average pore size distributions of the membrane were obtained from a nitrogen adsorption/desorption isotherm using a Micromeritics Tristar 3000 model. Pore diameters were estimated via the Barret–Joyner–Halenda (BJH) model [27]. The ASTM C20-00 standard was followed for the porosity tests of the support. Density was determined using an Accupic 1330 helium pycnometer. Thermogravimetric analysis (TGA) and differential scanning calorimetry (DSC) (Mettler Toledo TGA/DSC 1) were performed with 8.2587 mg of powder at a rate of 1°C/min, under air. The spectroscopic characterizations of raw bovine bone powder, calcined at 800°C, and synthetic HAP were investigated via Fourier transform infrared analysis (Varian FTS 1000 FT-IR, Mid-IR spectral range, cooled DTGS detector, Scimitar series, Varian Inc.). The chemical compositions of the raw bovine bone powder, synthetic hydroxyapatite and calcined bovine bone powder at 800°C were determined by X-ray fluorescence. The microstructures of the samples were studied using a scanning electron microscope (Bruker Nano XFlash Detector 5010 Energy Dispersive X-ray Microanalysis (EDX) System). The mechanical strength (modulus of rupture) was measured by a three-point bending flexural test with an Instron 5500 R universal testing machine with a 10-tonne capacity using Instron Blue Hill software.

### 2.6. Filtration tests and effluent characterization

Filtration tests were performed with a pharmaceutical effluent collected from SIMED, a pharmaceutical laboratory located in Sfax (Tunisia), using a laboratory-scale filtration system (Fig. 3a). This system was made of stainless steel to avoid corrosion problems and pressure was applied with $N_2$ gas. The membrane was placed in a 6 cm-diameter flat disk resulting in a filtration area of 0.0028 $m^2$ (Fig.3b). The supports were first conditioned by immersing them in ultrapure water for 24 h. They were then placed in the membrane housing and the system was filled with water from the top setting the temperature at 25°C. The pure water permeability of the support was calculated by filtrating distilled water.

The physicochemical parameters and the metal ion content of the raw wastewater was previously determined in order to evaluate the performance of the membrane in removing pollutants. The flux of the pharmaceutical effluent through the membrane was measured at different pressures (0.5, 1.0, 1.5, 2.0, 2.5 and 3.0 bar) and the permeability was calculated from the flux of each pressure.


Fig. 3. (a) Laboratory filtration set-up and (b) flat disk membrane.

The permeate was collected and characterized every 30 min for 3 h at a constant transmembrane pressure of 3.0 bar. The permeate physicochemical parameters included pH, turbidity, chemical oxygen demand (COD), biochemical oxygen demand for 5 d ($BOD_5$), and conductivity.

Turbidity was measured by a turbidimeter (Hach Ratio 2100A, USA) in accordance with standard method 2130B. Conductivity and pH measurements were performed using a conductometer (Istek EC-400L, USA) and a pH meter (Istek pH-220L, Japan), respectively. Chemical oxygen demand (COD) and biochemical oxygen demand for 5 d ($BOD_5$) were estimated by the colorimetric method (Fisher Bioblock Scientific reactor COD 10119, Japan) and WTW OxiTop®-i IS 6 BOD Measurement System 6 Place, Germany), respectively. The metal ion content was determined by inductively coupled plasma atomic emission spectroscopy (ICP-AES) (Agilent 4200 MP-AES, USA).

## 3. Results and discussion

### *3.1. Analysis of the raw bovine bone material and synthetic hydroxyapatite (HAp)*

Table 1 shows the chemical analysis report of the raw bovine bone powder, calcined bovine bone powder at 800°C, and synthetic hydroxyapatite. Calcium (Ca) and phosphorus (P) are seen to be present in high concentrations along with small amounts of chloride. The composition of bovine bone calcined at 800°C is found to be very similar to synthetic hydroxyapatite.

The XRD pattern shows the main phase of apatite and is indexed in the hexagonal system with a P63/m space-group (Fig. 4). However, the starting particle size of the raw materials in the ceramic process influences the sintering temperature to be used to obtain the required pore size.

The calcination temperature and particle size of bovine bone affect the composition, crystallinity, and crystallite size of the extracted natural HAp. The crystallinity of the HAp phase in bovine bone increases with increasing annealing temperature [28]. The crystallite size of bovine bone calcined at 800°C was calculated by the Sherrer formula, giving a crystallite size of 27.74 nm.

The granulometric analysis shows that the calcined bovine bone powder has a particle size distribution between 12.91 and 339.9 μm and the $d_{50}$ was 79.08 μm (Fig. 5). Moreover, the specific surface area was 2.6292 $m^2/g$.

The DSC-TGA data of a synthetic hydroxyapatite sample and bovine bone powder are represented in Fig. 6. The DSC results show an endothermic peak at 90°C followed by a strong exothermic peak with a maximum peak at around 335°C and a shoulder at around 420°C for raw bovine bone and synthetic HAp. Therefore, the same loss at the same temperature for the two samples were obtained from the TGA analyses. Four successive stages of weight loss can be observed in the TGA curves. The first loss below 200°C is attributed to bone dehydration (surface water), the second, between 200°C and 400°C, corresponds to a departure of structural water, the third between 400°C and 600°C is due to the combustion of the organic components of bone, and the fourth and final loss appears above 600°C mainly as a result of the release of $CO_2$ from the apatite network, which is due to the decomposition of carbonates [15,29].

Fig. 7 illustrates the FTIR spectra of raw bovine bone powder, calcined at 800°C and synthesized HAp samples. The spectrum of uncalcined and calcined bovine bone at 800°C have different profiles due to changes during heat treatment. The increase in the calcination temperature generates a product that is similar to the HAp structure, and which is deprived of carbonate groups. Through visual observation, the colour of the bone particles changes from yellowish-white to white after calcination. This colour change involves the breakdown of an organic substance (e.g., protein and collagen) in the heated bone powder [26,30]. The FTIR band at 1,650 $cm^{-1}$, which corresponds to the amide I of the collagen [23], is seen to be totally eliminated in the calcined samples.

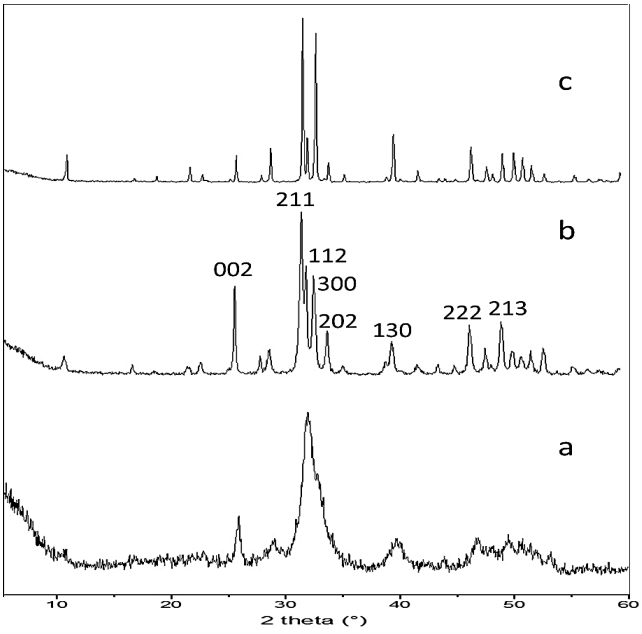


Fig. 4. X-ray diffractograms of (a) the raw bovine bone, (b) calcined bovine bone powder at 800°C, and (c) synthetic hydroxyapatite.

Table 1
Chemical composition (weight %) of the natural hydroxyapatite, raw and calcined, and synthetic hydroxyapatite

| Material | Bal. | Zr | Sr | Zn | $SiO_2$ | Ca | K | P | Si | Cl | S | Mg |
|---|---|---|---|---|---|---|---|---|---|---|---|---|
| Raw bovine bone | 64.6 | 0.0004 | 0.03 | 0.006 | 0.1 | 24.1 | 0.01 | 10.2 | 0.06 | 0.05 | 0.04 | 0.8 |
| Calcined bovine bone | 46.5 | 0.0003 | 0.003 | 0.001 | 0.0002 | 37.8 | – | 15.7 | – | 0.01 | – | – |
| Synthetic hydroxyapatite | 49.0 | 0.001 | 0.05 | 0.005 | 0.06 | 35.6 | – | 14.5 | – | 0.05 | – | 0.6 |

Balance: Difference to 100% of the sum of all measured elements.

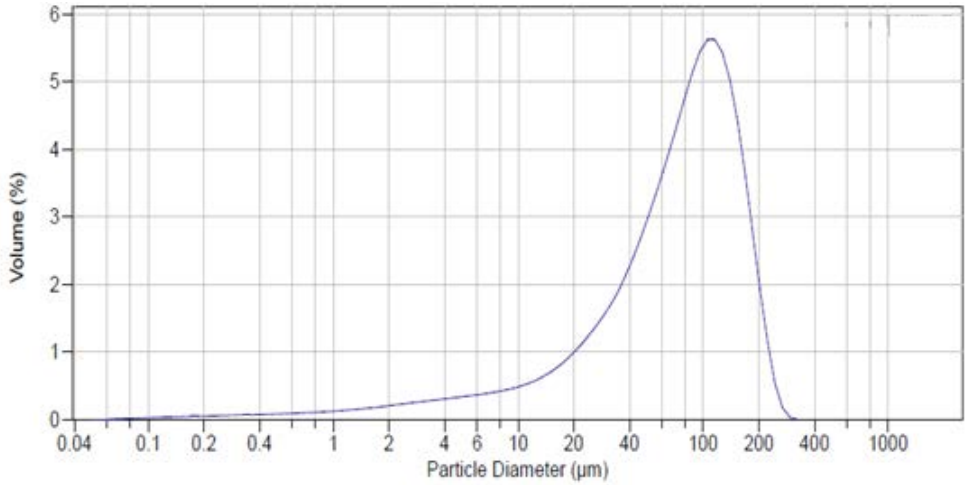


Fig. 5. Particle size distributions of calcined bovine bone powder.

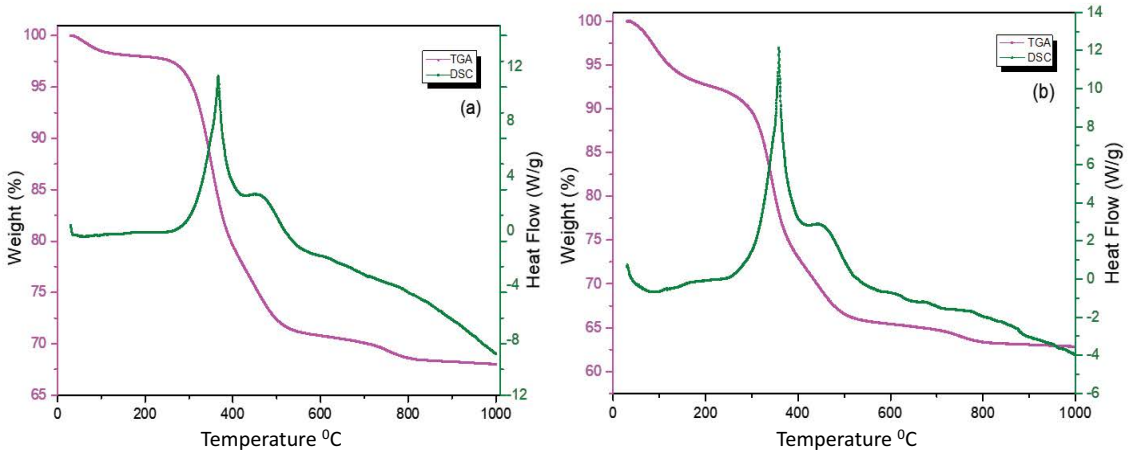


Fig. 6. Thermal analysis curves: DSC and TGA of (a) synthetic hydroxyapatite and (b) bovine bone powder.

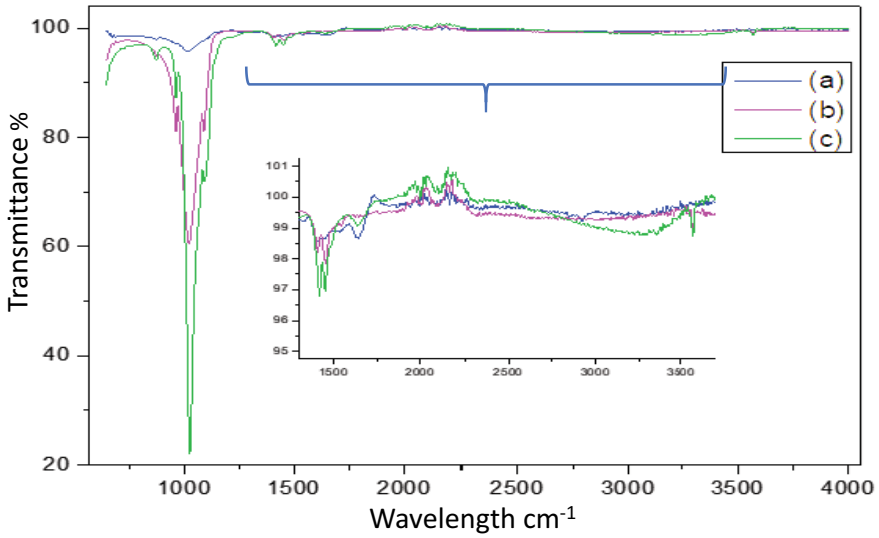


Fig. 7. FTIR spectra of (a) raw bovine bone powder, (b) bone powder calcined at 800°C, and (c) synthetic HAp. Amplification of the spectra in the 1,200 to 3,500 $cm^{-1}$ range (centre of the figure).

A strong and broad band that appears at 1,013; 1,022 and 1,087 $cm^{-1}$ in the calcined bone particles is associated with the phosphate group as well as the peak at 962 $cm^{-1}$. With increasing temperature the peak at 1,429 $cm^{-1}$ in the spectrum of raw bovine bone powder, which is attributed to the carbonate group, gradually decreases. The broad band at 3,572 $cm^{-1}$ is associated with the hydroxyl group, proving the presence of the hydroxyapatite phase [25,29].

Fig. 8 shows the SEM micrographs of the raw bovine bone powder before and after calcination at 800°C and of synthetic HAp powder. The particles of raw bovine bone powder have irregular shapes, including small spheres and rods, as do those of the calcined bone powder, in agreement with a previous report [30] (Fig. 8a). The average particle size of raw bovine bone is 304.285 µm (Fig. 8b). Moreover, calcinated bone powder presents more agglomerations due to the van der Waals attraction between the HAp particles during calcination [31]. Morphological variations were observed as the calcination temperature increased affecting the grain size and the porosity of the bone powder (Fig. 8c). While raw bovine bone particles present a highly dense micro surface, calcined bone particles contain multiple pores created by the decomposition of organic substances. Additionally, higher calcination temperatures led to an increase in the grain size associated with the heat energy absorbed by the particles [30].

The morphology of synthetic HAp is similar to that of the calcined bovine bone powder but its pore size is smaller (Fig. 8d).

### 3.2. Characterization of the membrane supports

#### 3.2.1. Scanning electron microscopy (SEM)

Fig. 9 illustrates the SEM images with the EDX spectrum of the membrane support. The EDX spectrum shows that

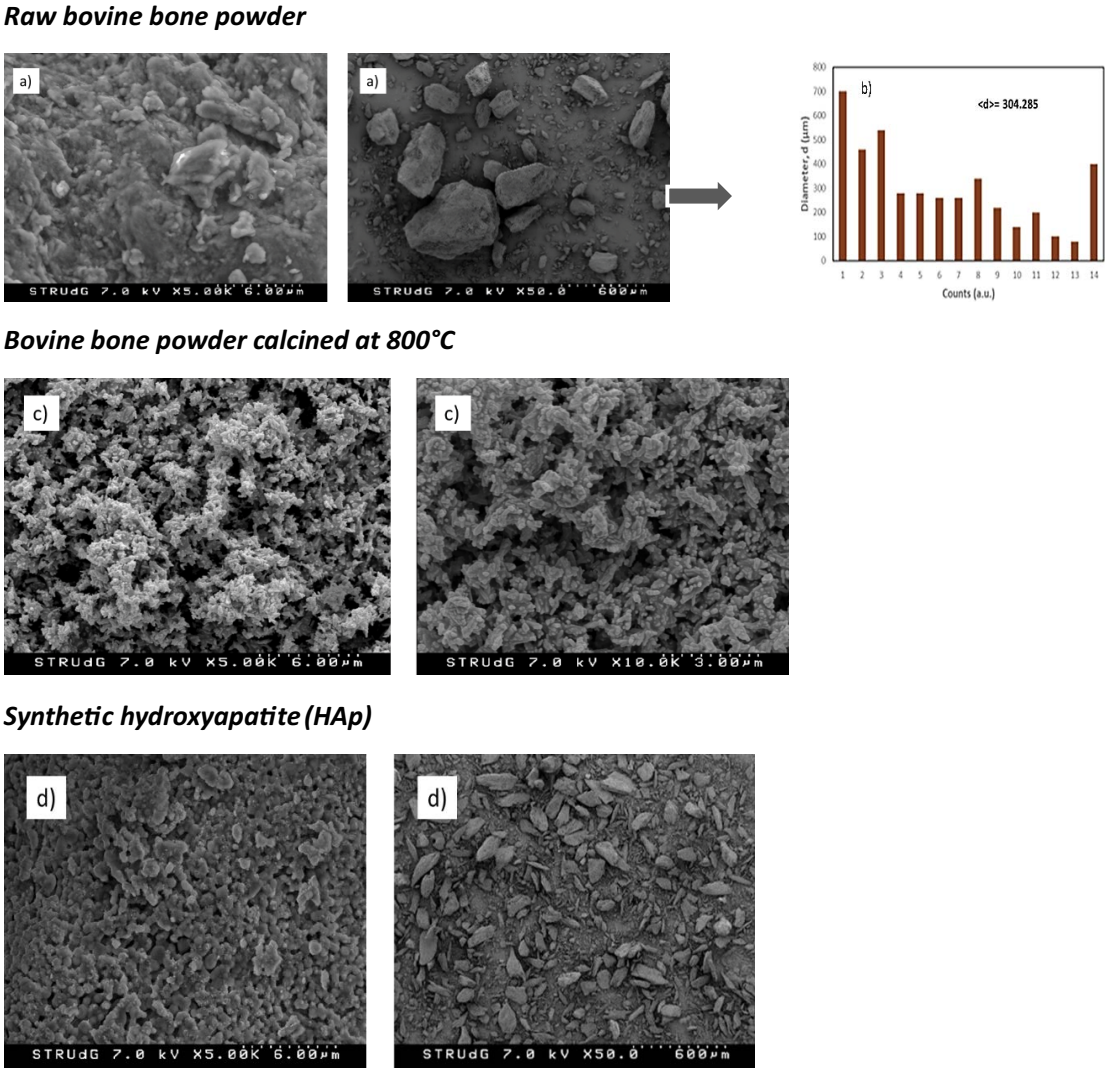


Fig. 8. SEM micrographs for: (a) raw bovine bone powder without thermal treatment at 50,000x, (b) average particle size of raw bovine bone, (c) bovine bone powder calcined at 800°C at 5,000x and 10,000x, and (d) synthetic hydroxyapatite (HAp) at 5,000x and 50x.

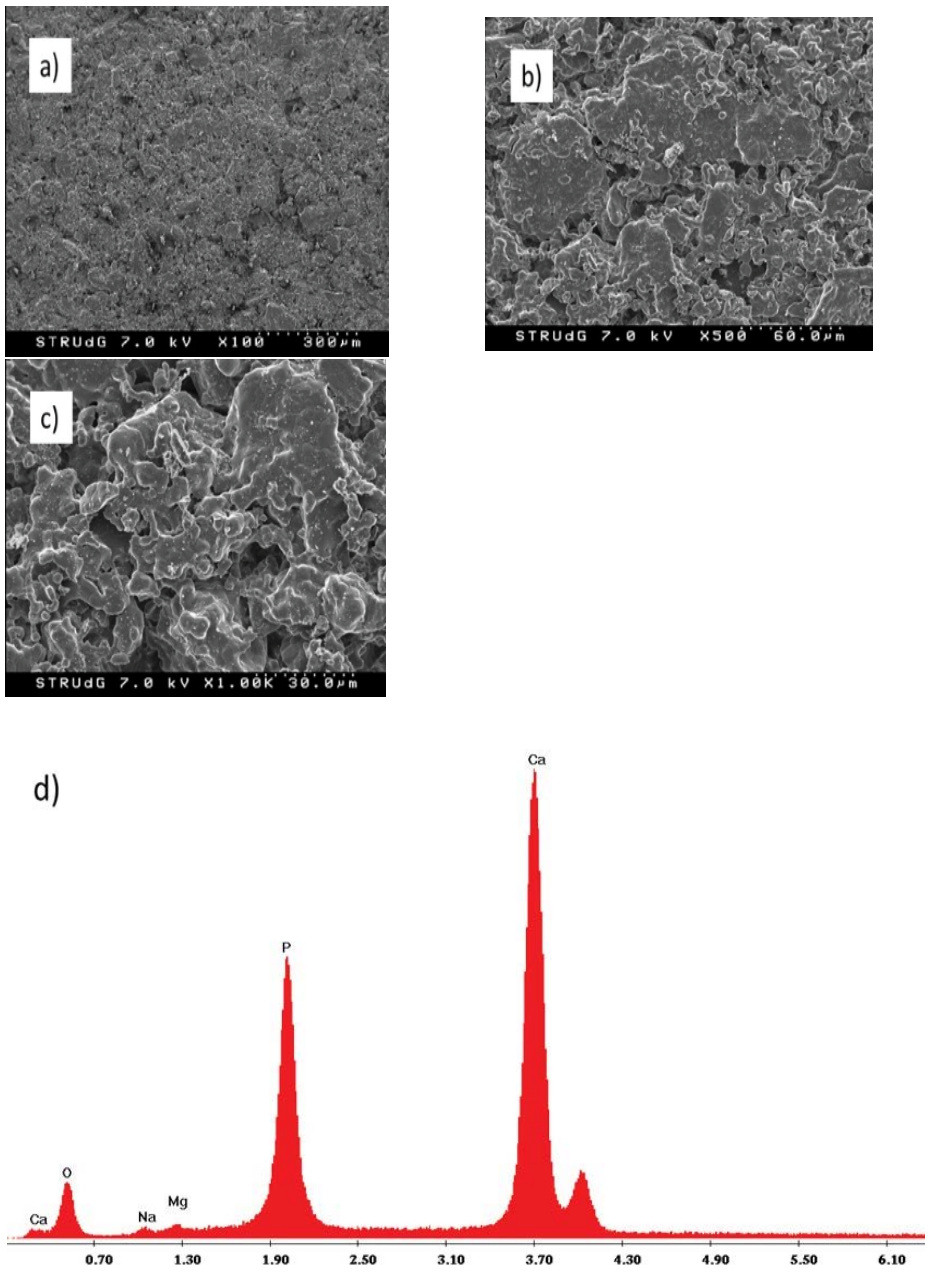


Fig. 9. SEM images of the membrane support sintered at 1,350°C at (a) 100x, (b) 500x, (c) 1,000x, and (d) EDX spectrum.

the intensity of phosphorus and calcium signals are much higher than other elements, such as oxygen, magnesium, and sodium.

### 3.2.2. Pore size determination

The adsorption and desorption isotherms of $N_2$ at 77 K (Fig. 10a) show a type IV isotherm according to IUPAC, indicating the presence of mesoporous (diameter of 2–50 nm) in the bovine bone membrane sintered at 1,350°C. The pore size distribution of the ultrafiltration bovine bone membrane was calculated by the Barrett, Joyner and Halenda (BJH) adsorption model [27]. Fig. 10b represents the log differential pore volume distribution curve ($dV/d\log D$) vs the pore diameter, where the largest peaks are between 11.5 and 32 nm. The mean pore diameter was 20 nm, confirming the ultrafiltration domain of the membrane.

### 3.2.3. Mechanical resistance

The mechanical resistance of the supports was also assessed and measured by the three-point mechanical test (Lloyd Instrument) applied to sintered parallelepiped test bars. Fig. 11 shows the evolution of the maximum fracture stress, σ (MPa), as a function of the sintering temperature (900, 1,100 and 1,350°C). The increase of σ with temperature

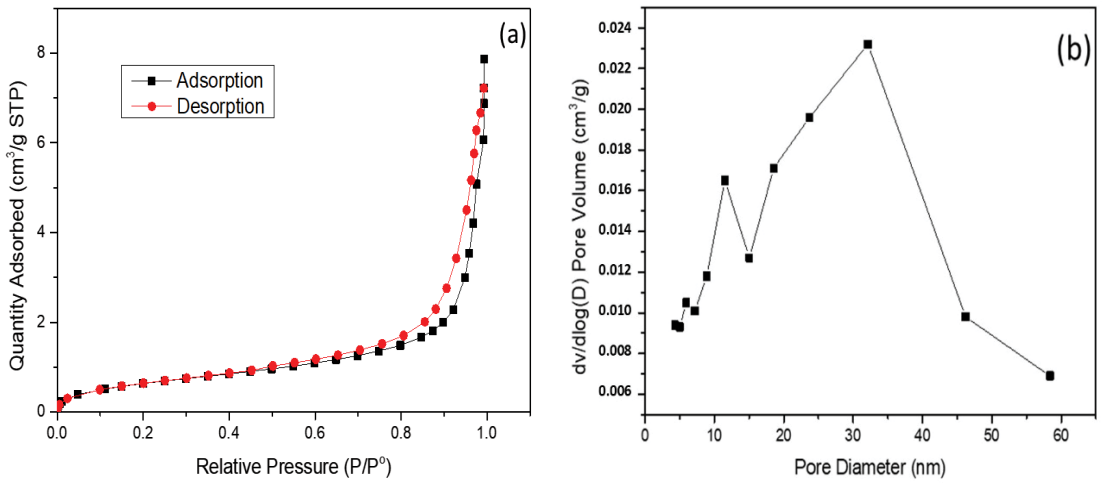


Fig. 10. (a) Nitrogen adsorption–desorption isotherm of bovine bone membrane sintered at 1,350°C and (b) pore-size distribution.

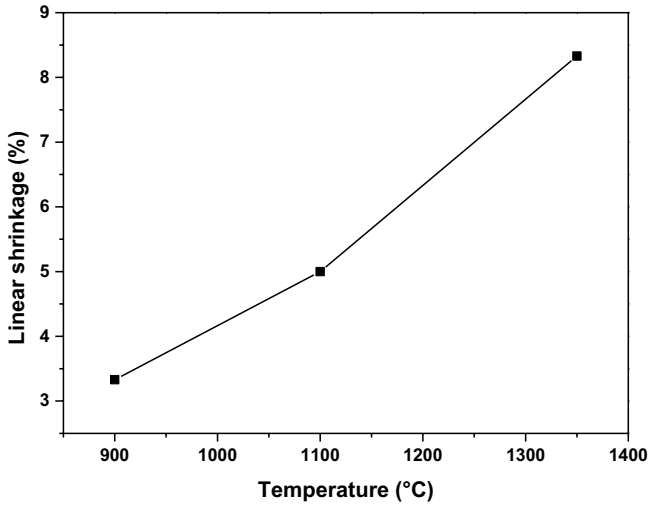


Fig. 11. Linear shrinkage vs. sintering temperature at 900°C, 1,100°C and 1,350°C.

resulted in the membrane acquiring progressively greater mechanical resistance.

The maximum rupture strength $\sigma_r$ (MPa) was calculated by following the elasticity theory [32]:

$$\sigma = \frac{2P_{max}}{\pi LD} \quad (1)$$

where $L$ (mm) and $D$ (mm) are the sample length and diameter, respectively. $P_{max}$ (N) is the maximum applied load at failure. Three samples of the material sintered at the same temperature were tested and an average value was then calculated.

The results in Table 2 show that the membrane support sintered at 900°C exhibited the lowest mechanical strength of 1.5 MPa. On the other hand, the membrane support sintered at 1,100°C had a mechanical strength of 3.5 MPa. The mechanical strength of the membrane support significantly increased to 16.1 MPa when the sintering temperature was further increased to 1,350°C.

Table 2
Mechanical strength at different temperatures ($n$ = 3)

| Temperature (°C) | 900 | 1,100 | 1,350 |
|---|---|---|---|
| Mechanical strength (MPa) | 1.5 ± 0.15 | 3.5 ± 0.25 | 16.1 ± 2 |

### 3.2.4. Linear shrinkage

It is generally accepted that linear shrinkage is mainly due to the burn out of the organic additives and the loss of moisture [33]. Hence, the shrinkage behaviour of the samples sintered at different temperatures was studied.

The linear shrinkage S (%) was calculated by measuring the membrane diameter before and after sintering with calliper's (precision: 0.01 mm) and using Eq. (2):

$$S = \frac{(D_0 - D)}{D_0} \times 100 \quad (2)$$

where $D_o$ is the membrane diameter before sintering and $D$ is the membrane diameter after sintering.

In Fig. 11 an increase in the sintering temperature from 900 to 1,350°C leads to a linear increase from 3.33% to 8.33%, in the shrinkage of the membrane. This linear relationship could be explained by the weight losses recorded in the TGA/DTA plots, which were assigned to dehydration of the material, burn out of organic matter, and chemical reactions.

### 3.2.5. Determination of membrane support water permeability

Water permeability was measured using the laboratory scale filtration set-up (Fig. 3). The permeate flux ($J_w$) was determined using Eq. (3):

$$J_w = \frac{V}{A \times t} \quad (3)$$

where $t$ is the time needed to collect a fixed volume of permeate, $V$ is the volume of permeate collected during time $t$, and $A$ is the effective area of the membrane. The permeability

was calculated from the slope of the permeate flux vs. the transmembrane pressure [Eq. (4)]:

$$J_w = L_p \times \Delta P \quad (4)$$

Firstly, the filtration performance of the membrane was characterized by determining its pure water permeability. The membrane support is conditioned by immersion in ultrapure water for a minimum of 24 h before filtration tests. Fig. 12 shows the linear increase in the permeate flux as the transmembrane pressure increased, resulting in a permeability of 470.49 L/h·m²·bar.

### 3.2.6. Chemical resistance

The chemical resistance of the membrane support sintered at 1,350°C to acidic and basic media was tested at room temperature for 30 d. Fig. 13 shows the weight loss variation as a function of time. The results show greater chemical resistance to acidic conditions (total weight loss of 1.86%) than to basic media (total weight loss of 9.15%).

### 3.2.7. Ultrafiltration of pharmaceutical industrial waste

The performance of the bovine bone membrane in the filtration of a pharmaceutical effluent was evaluated at a TMP of 3 bar and at 25°C. The pollutant retention $R$ through the membrane was calculated using the Eq. (5):

$$R(\%) = \left(1 - \left(\frac{C_p}{C_f}\right) \times 100\right) \quad (5)$$

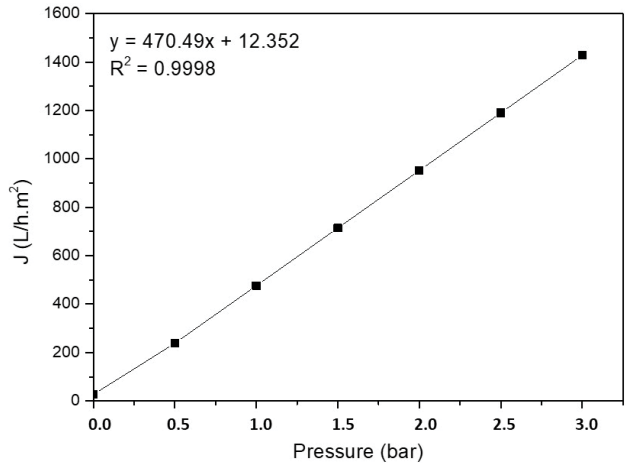


Fig. 12. Effect of pressure variation on permeate fluxes.

where $C_f$ and $C_p$ represent the concentrations of pollutants in the effluent and the permeate, respectively.

The variation in the pollutant concentrations was assessed by measuring the main physicochemical parameters of wastewater (Table 3). A quantitative retention of 97% was obtained for turbidity whereas COD retention was 73%. Conductivity and $BOD_5$ decreased by around 48.15% and 42%, respectively, and the iron and zinc contents decreased by 99.3% and 75.6%, respectively. In Fig. 14

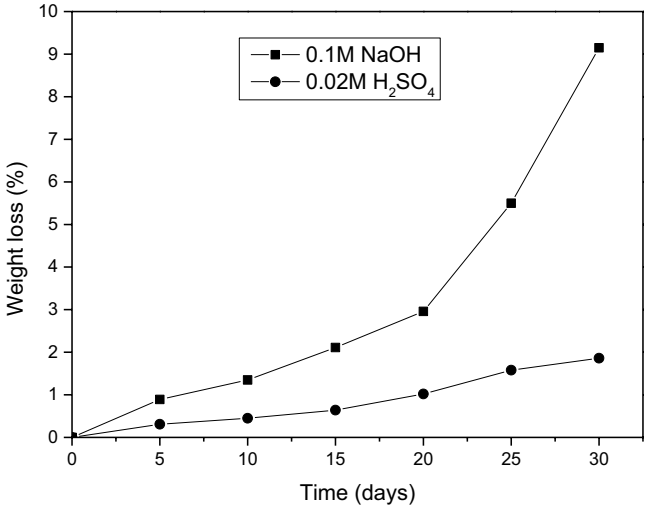


Fig. 13. Weight loss of biomaterial support sintered at 1,350°C in acidic and basic media as a function of time.

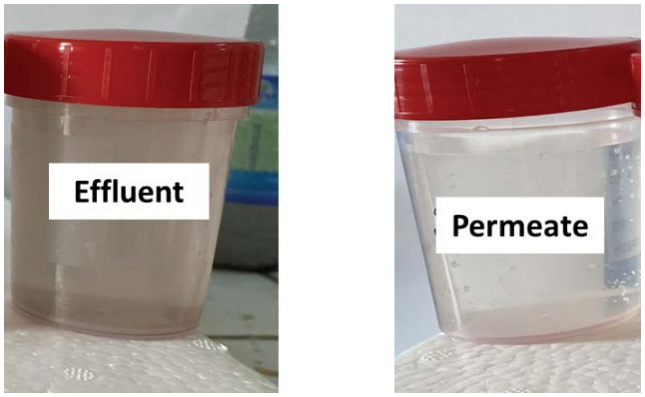


Fig. 14. Picture of the pharmaceutical wastewater before and after filtration ($P$ = 3 bar).

Table 3
Composition of the raw and treated effluents using bovine bone membrane

| | pH | Conductivity (mS/cm) | Turbidity (NTU) | COD (mg/L) | $BOD_5$ (mg/L) | Metal ions (mg/L) |
|---|---|---|---|---|---|---|
| Raw effluent | 7.23 | 2.15 | 176 | 585 | 70 | Fe 1.4; Zn 0.164; Cd, Cu < 0.01 |
| Filtrated with hydroxyapatite bone membrane ($T$° = 25°C, $P$ = 3bar) | 7.7 | 0.54 | 4.30 | 156.46 | 40 | Fe 0.01; Zn 0.04 |
| Retention rate (%) | – | 48.15 | 97 | 73 | 42 | Fe 99.3%; Zn 75.6% |

the permeate looks transparent and clean in comparison to the effluent. These results suggest that this kind of membrane may be efficient in the treatment of a broad range of wastewaters.

In this study we have shown that the bio-ceramic ultrafiltration membrane that we have prepared here is effective in reducing the general physicochemical parameters of wastewater and removing metal ions such as iron and zinc that were present at low concentrations.

Several studies in the literature have reported the sorptive properties of hydroxyapatite and hydroxyapatite-based materials in the removal of heavy metals, including Pb, Cu, Zn, Sr, and Fe [25,34]. A hydroxyapatite-based bio-ceramic hollow-fibre membrane was also found to eliminate metal ions at low concentrations from textile industry effluents, showing the possibility of combining the filtration capacity of the bio-membrane with the ion-exchange properties of HAp to enhance the potential of these membranes [25].

## 4. Conclusions

In this study, a hydroxyapatite bio-ceramic membrane has been successfully developed for the filtration of wastewater. Bio-hydroxyapatite powder was obtained from raw bovine bones by a thermal method. The bio-ceramic membrane prepared with 92 wt.% bovine bone powder and 8 wt.% additives at the sintering temperature of 1,350°C has an average pore size of 20 nm, a high mechanical strength (16.1 Mpa) and high chemical resistance. The chemical composition, structure and particle size of the bio-hydroxyapatite powder and of the flat membrane were characterized by different techniques. The bio-ceramic ultrafiltration membrane showed its potential to treat wastewater with a stable flux of 470.49 $L \cdot h \cdot m^2 \cdot bar$ and excellent performance in removing both contaminants (COD = 73%, $BOD_5$ = 42%, turbidity = 97%, conductivity = 48.15%) and heavy metals (Fe = 99.3%, Zn = 75.6%). The development of hydroxyapatite-based bio-ceramic membranes is a cost-effective alternative to commercial ceramic membranes, allowing the valorization of waste animal bones. In addition to the sieving mechanism, which is related to the pore size of the membrane, the sorptive properties of bio-hydroxyapatite towards metal ions and other pollutants will contribute to improving the separation performance of bio-ceramic membranes. Further investigations into the hydroxyapatite-based membrane adsorption mechanism and membrane stability are required for future development of bio-ceramic membranes.

## Acknowledgements

This study was financed by the project "Valorisation des os bovin pour l'élaboration des membranes de micro et nano-filtrations à base de biomatériaux pour la dépollution des eaux usées", PAQ-PAES of the Laboratory of Material Sciences and Environment, Faculty of Sciences of Sfax, University of Sfax, Tunisia and by the Ministerio de Ciencia, Innovacion y Universidades (MCIU) through project PID2019-107033 GB-C22/AEI/10.13039/501100011033.

## References

[1] C. Castel, E. Favre, Membrane separations and energy efficiency, J. Membr. Sci., 548 (2018) 345–357.
[2] J. Usman, M.H.D. Othman, A.F. Ismail, M.A. Rahman, J. Jaafar, Y.O. Raji, A.O. Gbadamosi, T.H. El Badawy, K.A.M. Said, An overview of superhydrophobic ceramic membrane surface modification for oil-water separation, J. Mater. Res. Technol., 12 (2021) 643–667.
[3] N. Abdullah, N. Yusof, W.J. Lau, J. Jaafar, A.F. Ismail, Recent trends of heavy metal removal from water/wastewater by membrane technologies, J. Ind. Eng. Chem., 76 (2019) 17–38.
[4] S. Khadijah Hubadillah, M. Riduan Jamalludin, M.H Dzarfan Othman, Y. Iwamoto, Recent progress on low-cost ceramic membrane for water and wastewater treatment, Ceram. Int., 48 (2022) 24157–24191.
[5] W. Li, H. Dong, H. Yu, D. Wang, H. Yu, Global characteristics and trends of research on ceramic membranes from 1998 to 2016: based on bibliometric analysis combined with information visualization analysis, Ceram. Int., 44 (2018) 6926–6934.
[6] I. Kammakakam, Z. Lai, Next-generation ultrafiltration membranes: a review of material design, properties, recent progress, and challenges, Chemosphere, 316 (2023) 137669, doi: 10.1016/j.chemosphere.2022.137669.
[7] Y. Guesmi, R. Lafi, H. Agougui, M. Jabli, A. Oun, S. Majumdar, A. Hafiane, Synthesis and characterization of alpha alumina-natural apatite based porous ceramic support for filtration application, Mater. Chem. Phys., 239 (2020) 122067, doi: 10.1016/j.matchemphys.2019.122067.
[8] S. Lakshmi Sandhya Rani, R. Vinoth Kumar, Fabrication and characterization of ceramic membranes derived from inexpensive raw material fuller's earth clay, Mater. Sci. Eng., B, 284 (2022) 115877, doi: 10.1016/j.mseb.2022.115877.
[9] S.L. Sandhya Rani, R.V. Kumar, Insights on applications of low-cost ceramic membranes in wastewater treatment: a mini-review, Case Stud. Chem. Environ. Eng., 4 (2021) 100149, doi: 10.1016/j.cscee.2021.100149.
[10] I. Barrouk, S. Alami Younssi, A. Kabbabi, M. Persin, A. Albizane, S. Tahiri, New ceramic membranes from natural Moroccan phosphate for microfiltration application, Desal. Water Treat., 55 (2015) 53–60.
[11] N. Saffaj, M. Persin, S.A. Younsi, A. Albizane, M. Cretin, A. Larbot, Elaboration and characterization of microfiltration and ultrafiltration membranes deposited on raw support prepared from natural Moroccan clay: application to filtration of solution containing dyes and salts, Appl. Clay Sci., 31 (2006) 110–119.
[12] P. Belibi, S. Cerneaux, M. Rivallin, N. Martin, M. Cretin, Elaboration of low-cost ceramic membrane based on local material for microfiltration of particle from drinking water, J. Appl. Chem., 3 (2014) 1991–2003.
[13] H. Alghamdi, A. Dakhane, A. Alum, M. Abbaszadegan, B. Mobasher, N. Neithalath, Synthesis and characterization of economical, multi-functional porous ceramics based on abundant aluminosilicates, Mater. Des., 152 (2018) 10–21.
[14] B. Achiou, H. Elomari, M. Ouammou, A. Albizane, J. Bennazha, S.A. Younssi, I.E. El Amrani, A. Aaddane, Elaboration and characterization of flat ceramic microfiltration membrane made from natural Moroccan pozzolan (Central Middle Atlas), Eng. Mater. Sci., 7 (2016) 196–204.
[15] N. Saffaj, N. El Baraka, R. Mamouni, H. Zgou, A. Laknifli, S. Younssi Alami, Y. Darmane, M. Aboulkacem, O. Mokhtari, New bio ceramic support membrane from animal bone, J. Microbiol. Biotechnol. Res., 3 (2013) 1–6.
[16] W. Misrar, M. Loutou, L. Saadi, M. Mansori, M. Waqif, C. Favotto, Cordierite containing ceramic membranes from smectetic clay using natural organic wastes as pore-forming agents, J. Asian Ceram. Soc., 5 (2017) 199–208.
[17] H. De Teng, Q. Wei, Y.L. Wang, S.P. Cui, Q.Y. Li, Z.R. Nie, Asymmetric porous cordierite ceramic membranes prepared by phase inversion tape casting and their desalination performance, Ceram. Int., 46 (2020) 23677–23685.

[18] M. Mohamed, N. Dayirou, H. Mohamed, N. André, L.N. Gisèle Laure, N. Daniel, Effect of porogenic agent type and firing temperatures on properties of low-cost microfiltration membranes from kaolin, Trans. Indian Ceram. Soc., 79 (2020) 1–12.
[19] A. Agarwalla, K. Mohanty, Comprehensive characterization, development, and application of natural/Assam kaolin-based ceramic microfiltration membrane, Mater. Today Chem., 23 (2022) 100649, doi: 10.1016/j.mtchem.2021.100649.
[20] M. Purnima, T. Paul, K. Pakshirajan, G. Pugazhenthi, Onshore oilfield produced water treatment by hybrid microfiltration-biological process using kaolin based ceramic membrane and oleaginous *Rhodococcus opacus*, Chem. Eng. J., 453 (2023) 139850, doi: 10.1016/j.cej.2022.139850.
[21] A. El Azizi, A. Bayoussef, Ch. Bai, M. Abou-Salama, M. Mansori, R. Hakkou, M. Loutou, Development of clayey ceramic membranes prepared with bio-based additives: application in water and textile wastewater treatment, Ceram. Int., 49 (2023) 5776–5787.
[22] M.H. Santos, M. de Oliveira, L.P. de F. Souza, H.S. Mansur, W.L. Vasconcelos, Synthesis control and characterization of hydroxyapatite prepared by wet precipitation process, Mater. Res., 7 (2004) 625–630.
[23] N.A.M. Barakat, M.S. Khil, A.M. Omran, F.A. Sheikh, H.Y. Kim, Extraction of pure natural hydroxyapatite from the bovine bones bio waste by three different methods, J. Mater. Process. Technol., 209 (2009) 3408–3415.
[24] A.N.K. Ahmad Fara, M.A. Bin Yahya, H.Z. Abdullah, Preparation and characterization of biological hydroxyapatite (HAp) obtained from Tilapia Fish Bone, Adv. Mater. Res., 1087 (2015) 152–156.
[25] S.K. Hubadillah, M.H.D. Othman, Z.S. Tai, M.R. Jamalludin, N.K. Yusuf, A. Ahmad, M.A. Rahman, J. Jaafar, S.H.S.A. Kadir, Z. Harun, Novel hydroxyapatite-based bio-ceramic hollow fiber membrane derived from waste cow bone for textile wastewater treatment, Chem. Eng. J., 379 (2020) 122396, doi: 10.1016/j.cej.2019.122396.
[26] M. Sadat-Shojai, M.T. Khorasani, E. Dinpanah-Khoshdargi, A. Jamshidi, Synthesis methods for nanosized hydroxyapatite with diverse structures, Acta Biomater., 9 (2013) 7591–7621.
[27] C. Scherdel, G. Reichenauer, M. Wiener, Relationship between pore volumes and surface areas derived from the evaluation of $N_2$-sorption data by DR-, BET- and *t*-plot, Microporous Mesoporous Mater., 132 (2010) 572–575.
[28] C.Y. Ooi, M. Hamdi, S. Ramesh, Properties of hydroxyapatite produced by annealing of bovine bone, Ceram. Int., 33 (2007) 1171–1177.
[29] M. Figueiredo, A. Fernando, G. Martins, J. Freitas, F. Judas, H. Figueiredo, Effect of the calcination temperature on the composition and microstructure of hydroxyapatite derived from human and animal bone, Ceram. Int., 36 (2010) 2383–2393.
[30] W. Khoo, F.M. Nor, H. Ardhyananta, D. Kurniawan, Preparation of natural hydroxyapatite from bovine femur bones using calcination at various temperatures, Procedia Manuf., 2 (2015) 196–201.
[31] N. Bano, S.S. Jikan, H. Basri, S. Adzila, A.H. Nuhu, Natural hydroxyapatite extracted from bovine bone, Sci. Technol. J., 9 (2017) 22–28.
[32] M.H. Sadd, Elasticity: Theory, Applications and Numerics, 2nd ed., Elsevier, New York, 2009.
[33] G.C.C. Yang, C.M. Tsai, Effects of starch addition on characteristics of tubular porous ceramic membrane substrates, Desalination, 233 (2008) 129–136.
[34] R.I. Brazdis, I. Fierascu, S.M. Avramescu, R.C. Fierascu, Recent progress in the application of hydroxyapatite for the adsorption of heavy metals from water matrices, Materials, 14 (2021) 6898, doi: 10.3390/ma14226898.